

Cite this: *Chem. Sci.*, 2025, 16, 7551

All publication charges for this article have been paid for by the Royal Society of Chemistry

# Transforming 2D azolium salts to 3D caged tertiary amines *via* stereoselective dearomative cascade annulation†

Koushik Patra,<sup>a</sup> Samiran Deb,<sup>a</sup> Venkata Surya Kumar Choutipalli,<sup>c</sup> Sana Mulani,<sup>a</sup> Sumitava Mallik,<sup>a</sup> Venkatesan Subramanian<sup>bc</sup> and Mahiuddin Baidya<sup>\*,a</sup>

Three-dimensional fused-ring frameworks, especially those incorporating heteroatoms, are fundamental to expanding chemical space and unlocking unique properties critical for drug discovery and functional materials, yet their synthesis remains a formidable challenge. Herein, we report for the first time the union of two distinct azolium salts as an efficient synthetic platform to access tertiary amine-caged frameworks under mild conditions. The strategy combines the masked nucleophilic and electrophilic properties of isoquinolinium and pyridinium salts, and avails double dearomatization guided inverse electron demand (4 + 2) or (3 + 2) annulation in a highly regio- and diastereoselective manner to construct the nitrogen caged motifs. Our methodology creates two new rings and four new bonds in a single operation and transforms flat-aromatic compounds into structurally unprecedented three-dimensional architectures with contiguous stereocenters in very high yields. DFT studies have shed light on the reaction mechanism, indicating that the annulation step is rate-limiting, with (4 + 2) annulation proceeding stepwise and (3 + 2) annulation following a concerted pathway.

Received 26th February 2025

Accepted 25th March 2025

DOI: 10.1039/d5sc01527h

rsc.li/chemical-science

## Introduction

Transforming two-dimensional (2D) molecular frameworks into three-dimensional (3D) architectures by incorporating out-of-plane substituents can elevate the fraction of sp<sup>3</sup> atoms (F sp<sup>3</sup>) in the resulting structures.<sup>1</sup> This enhancement is a crucial design element in drug development, contributing to improved clinical outcomes such as better solubility, enhanced receptor-ligand interactions, target selectivity, and efficacy.<sup>1,2</sup> In this context, tertiary amine-containing caged-like molecular structures offer exciting possibilities in pharmaceutical science and synthetic chemistry (Scheme 1a).<sup>3</sup> They serve as fundamental backbones for various bioactive natural products, and many derivatives find widespread application as reagents, ligands, and catalysts in organic synthesis.<sup>3,4</sup> Therefore, developing cogent strategies towards these intriguing, structurally complex caged-amine frameworks from readily available starting materials through simple experimental procedures is highly desirable.<sup>5</sup>

The aromatic heterocycles, specifically N-heterocycles, are inexpensive building blocks and widely available in great structural diversity.<sup>6</sup> We envisioned transforming these flat two-dimensional molecules into three-dimensional architectures as a synthetic maneuver to access tertiary amine caged-like frameworks. This strategic blueprint involves a dearomatization reaction, which is fundamental in the construction of diverse molecular scaffolds in organic synthesis;<sup>7</sup> however, literature precedent is rare in the production of tertiary amine caged-like frameworks. The pioneering examples from Gin and co-workers showcasing the dearomatization of oxidoisoquinolinium and oxidopyridinium betaines stand alone in this realm as a direct and concise protocol (Scheme 1b).<sup>8a,b</sup> However, this strategy cannot be utilized with the less reactive parent isoquinolinium salt and is also restricted for intramolecular processes.<sup>8c-h</sup>

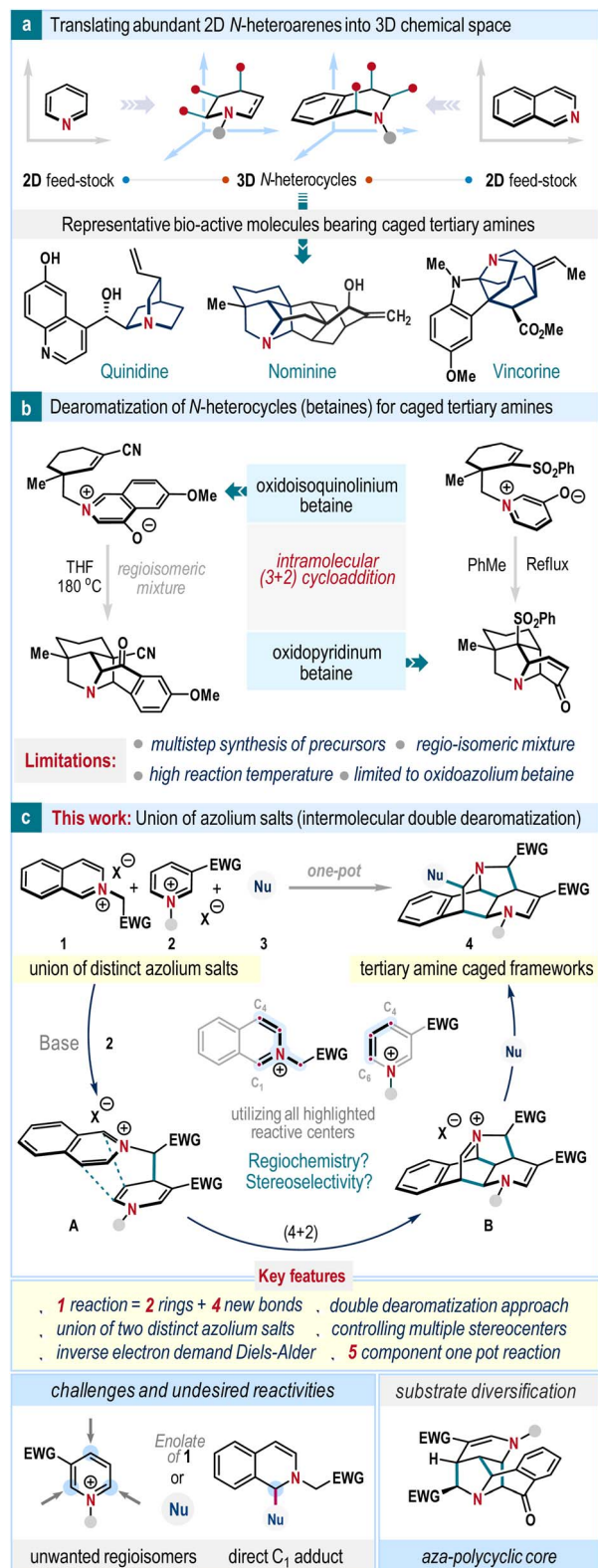
Nature often adopts the union of two or more simplified molecular progenitors in the form of cascade reactions to dispense complex architectures, which provide great impetus in devising biomimetic synthetic strategies.<sup>9</sup> We hypothesized that an assembly of isoquinolinium (**1**) and pyridinium salts (**2**) could be a convenient route to make tertiary amine caged-like frameworks (Scheme 1b). In the presence of a base, the enolate thus generated from isoquinolinium salt **1** can react with pyridinium salt **2** to give intermediate **A** which possesses all characteristics to expedite an intramolecular inverse electron demand Diels–Alder reaction. Subsequently, the iminium ion intermediate **B** will be formed, which upon quenching with

<sup>a</sup>Department of Chemistry, Indian Institute of Technology Madras, Chennai 600 036, Tamil Nadu, India. E-mail: mbaidya@iitm.ac.in

<sup>b</sup>Department of Chemistry, Indian Institute of Technology Madras, Chennai 600036, Tamil Nadu, India

<sup>c</sup>Centre for High Computing, CSIR-Central Leather Research Institute, Chennai 600020, Tamil Nadu, India

† Electronic supplementary information (ESI) available. CCDC 2190610. For ESI and crystallographic data in CIF or other electronic format see DOI: <https://doi.org/10.1039/d5sc01527h>



Scheme 1 Dearomatization strategies towards three-dimensional cage amine scaffolds.

a suitable nucleophile would furnish the desired tertiary amine caged scaffold **4**. This design is unique as it endorses the dearomatization event of both isoquinoline and pyridine

heterocycles in a one-pot operation, which is so far unexplored. Also, it maximizes the use of potential reactive sites of isoquinoline (C1, C3, and C4 centers) and pyridine (C4, C5, and C6 positions) heterocycles in a cascade fashion (Scheme 1b). However, the successful execution of this plan must overcome several challenges. The pyridinium salts **2** are prototypes of ambident electrophiles and accept nucleophilic attack at C2, C4, and C6 centers (Scheme 1b, below). Hence, maintaining high regioselectivity during this cascade event is imperative to facilitate the formation of the caged framework. Further, a judicious choice of nucleophile (Nu) is critical so that its direct reaction with pyridinium salt as well as isoquinolinium salt can be outcompeted. Also, mild reaction conditions is necessary to suppress the potential self-dimerization process of isoquinolinium salt **1** and achieve high diastereoselectivity as the successful cascade would embrace four new bond formations with contiguous stereocenters.

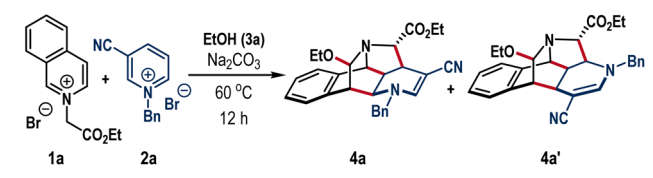
Herein, we report the development of this approach and demonstrate an unprecedented intermolecular annulative double dearomatization cascade of isoquinolinium and pyridinium salts to obtain tertiary cage amine scaffolds in high yields with excellent regio- and diastereoselectivity. Notably, the protocol can be performed as a one-pot five-component coupling without compromising efficacy and selectivity, highlighting synthetic versatility.<sup>10</sup> Through the substrate design, we have also showcased the synthesis of the central aza-polycyclic core of hetisine-type natural alkaloids. We also provide a detailed elucidation of the reaction mechanism, supported by DFT studies, offering valuable insights into this transformative process.

## Result and discussion

We began our investigation following the model reaction between isoquinolinium salt **1a** and pyridinium salt **2a** (Table 1). We consider ethyl alcohol as the reaction medium owing to its inability to undergo nucleophilic addition to azolum salts **1a** and **2a**; however, it could play the role of the third component and react with the proposed iminium intermediate to produce cage frameworks. Grounded on this understanding, a mixture of **1a** and **2a** in EtOH solvent was exposed to Na<sub>2</sub>CO<sub>3</sub> base at room temperature (entry 1).

To our satisfaction, the formation of the caged scaffold took place, albeit the reaction was sluggish to render the desired annulation product **4a** in 36% yield after 30 h. When the temperature was increased to 60 °C, the reaction was completed within 12 h, and product **4a** was isolated as a single diastereomer with an improved yield of 83% (entry 2). At this juncture, a minor amount of other regioisomer **4a'** (arising from the initial C6-attack on **2a** was also formed in 8% yield. Further increase of the reaction temperature rendered detrimental yield which can be attributed to the initiation of various undesired reactions as observed in the TLC (entry 3). The choice of solvent was crucial to preserve efficacy and selectivity. Examination of DCE, THF, and CH<sub>3</sub>CN solvents along with a reagent amount of EtOH provided an almost 1 : 1 mixture of **4a** and **4a'** with poor yields (entry 4). The reaction was



Table 1 Optimization of reaction conditions<sup>a</sup>


Entry	Deviation from the standard conditions	Yield of 4a <sup>b</sup> (%)	4a : 4a'
1	At rt for 30 h	36	—
2	None	83	>10 : 1
3	At 80 °C	70	>10 : 1
4 <sup>c</sup>	DCE/THF/CH <sub>3</sub> CN instead of EtOH	25/32/54	1 : 1
5	K <sub>2</sub> CO <sub>3</sub> /Li <sub>2</sub> CO <sub>3</sub> /Ag <sub>2</sub> CO <sub>3</sub> instead of Na <sub>2</sub> CO <sub>3</sub>	72/75/68	>10 : 1
6	DIPEA/GC/DBU instead of Na <sub>2</sub> CO <sub>3</sub>	77/64/41	>10 : 1
7	Without Na <sub>2</sub> CO <sub>3</sub>	—	—

<sup>a</sup> Reaction conditions: **1a** (0.24 mmol), **2a** (0.2 mmol), base (0.4 mmol), and EtOH (1.5 mL), 12 h, under N<sub>2</sub> atmosphere. <sup>b</sup> Isolated yields were provided. <sup>c</sup> Ethanol (0.24 mmol) was used. DCE: 1,2-dichloroethane, GC: guanidine carbonate.

productive with different inorganic bases such as Li<sub>2</sub>CO<sub>3</sub>, K<sub>2</sub>CO<sub>3</sub>, and Cs<sub>2</sub>CO<sub>3</sub> (entry 5). Organic bases also can promote this reaction. Hunig's base (iPr<sub>3</sub>NEt) and guanidine carbonate (GC) gave **4a** in 77% and 64% yields, respectively, while the reaction yield was reduced to 41% for DBU (entry 6). Nonetheless, the regioisomeric ratio remained >10 : 1 for all these cases. Notably, the reaction completely shut down in the absence of a base (entry 7). Compound **4a** was also crystalized and the single crystal X-ray analysis unambiguously confirmed the caged structure with defined regio- and stereoselectivity (Scheme 2, above).

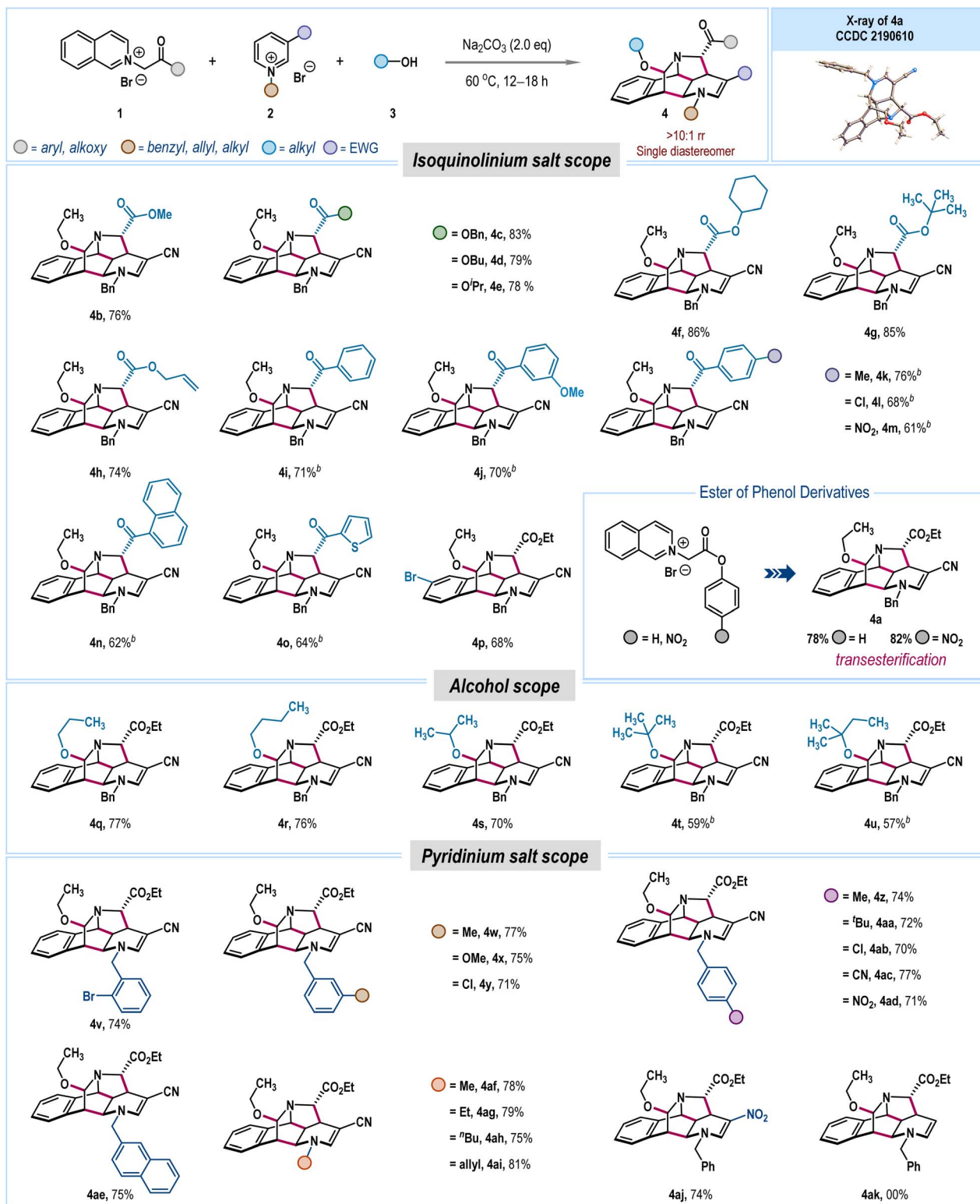
With the optimized reaction conditions (Table 1, entry 2), we then explored the substrate scope (Scheme 2). Initially, different isoquinolinium salts (**1**) were examined. Isoquinolinium salts obtained from various  $\alpha$ -bromo esters of primary (**4b–4d**), secondary (**4e**, **4f**), and tertiary (**4g**) alcohols smoothly delivered caged molecules in very high yields. The product with allyl ester **4h** was also obtained in 74% yield. Similarly, isoquinolinium salts prepared from phenacyl bromide and its derivatives having electron-donating and electron-deficient functionalities at *meta*- and *para*-positions in the aryl ring were suitable substrates to offer **4i–4m** in high yields. Also, substrates with bulky 1-naphthyl ketone and heterocyclic thienyl ketone motifs gave **4n** and **4o** in 62% and 64% yields, respectively. The bromine functional group in the isoquinoline ring (**4p**) can also be accommodated, leaving a synthetic handle for further transformation. The protocol was also effective with phenolic ester-embedded isoquinolinium salts; however, for these cases, we observed concomitant transesterification with ethanol solvent leading to **4a** in high yields (Scheme 2). The generality of other alcoholic solvents as a third component in this synthesis was also examined. Linear alcohols such as propanol, butanol, and branch alcohol isopropanol delivered **4q–4s** in 70–77% yields. With bulky alcohols, for example, tertiary butanol and *tert*-amyl alcohol, desired products **4t** and **4u** were isolated in good yields.

Next, the reaction scope was surveyed with different pyridinium salts **2** (Scheme 2). A wide variety of *N*-benzyl analogs of 3-cyanopyridinium salts bearing electronically different substitutions at *ortho*-, *meta*-, and *para*-positions of the aryl ring furnished tertiary amine caged compounds **4v–4ae** in uniformly high yields (70–77%). Reactions of *N*-methyl (**4af**), ethyl (**4ag**), butyl (**4ah**), and allyl (**4ai**) pyridinium salts also led to high annulation yields. The 3-nitropyridinium salt also readily participated in this reaction and the corresponding caged amine product **4aj** was isolated in 74% yield. It is worth noting that an activated pyridinium salt was essential for the synthesis of caged amine framework, while parent pyridinium salt without any activating group was not productive (**4ak**). Satisfyingly, all products were prepared as a single diastereomer with >10 : 1 regioselectivity.

To garner diversity in the synthesis, we employed 3-methyl substituted isoquinolinium salts **5**. We hypothesized that the presence of methyl group could be beneficial to neutralize the iminium ion intermediate **C** generating from the (4 + 2) annulation process and thereby a tertiary amine cage framework bearing an exocyclic double bond could be within reach (Scheme 3). Accordingly, isoquinolinium salt **5a** was reacted with pyridinium salt **2a** under standard reaction conditions where desired product **6** was formed in 57% yield. The combination of other isoquinolinium salts **5b** and **5c** with pyridinium salt **2a** was also fruitful, albeit the process was associated with a transesterification step leading to **6** in synthetically useful yields (Scheme 3).

As an alternative route to cage tertiary amine framework, we plan to alter the reaction modality from (4 + 2) annulation to (3 + 2) annulation. It was envisioned that incorporation of a suitable electron-donating functionality at the C4 position of isoquinolinium salt will increase the nucleophilic character at the C3 position and such a scenario is expected to favor (3 + 2) annulation towards desired cage framework (Scheme 4a). In view of that, isoquinolinium salt **7** having a methoxy group at C4

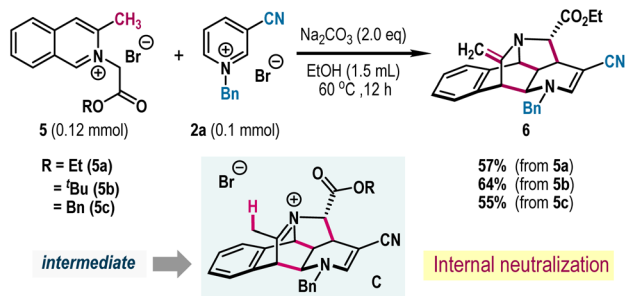




Scheme 2 Exploration of the reaction scopes. <sup>a</sup>Reaction conditions: **1** (0.24 mmol), **2** (0.2 mmol),  $\text{Na}_2\text{CO}_3$  (0.4 mmol), and alcohol solvent **3** (1.5 mL), under  $\text{N}_2$  atmosphere. Isolated yields were provided. <sup>b</sup>Reaction time was 18 h.

position was prepared and reacted with **2a** under standard reaction conditions. However, we observed formation of cage molecule **8** in 80% yield *via* (4 + 2) annulation discussed in the

preceding section, indicating further substrate modification was required (Scheme 4b). Accordingly, the reaction was revisited with isoquinolinium salt **9** bearing a free hydroxyl



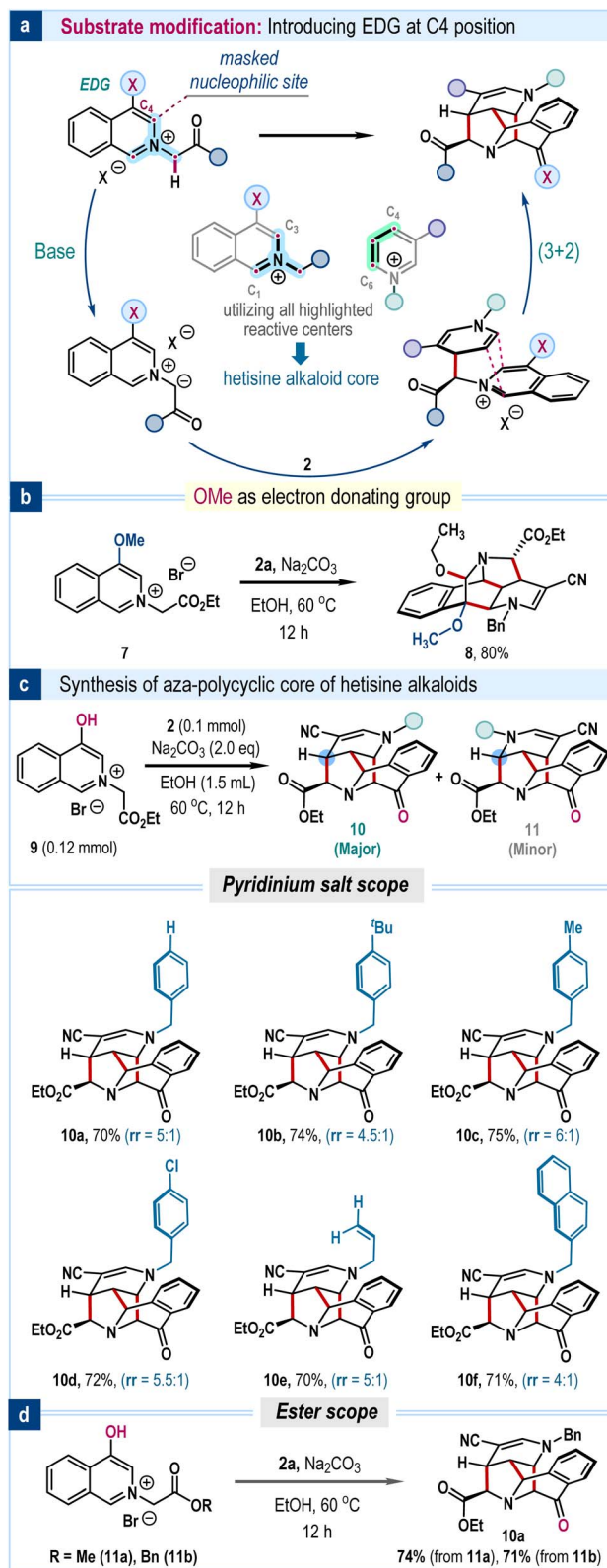
Scheme 3 Synthesis of cage tertiary amines with exocyclic double bond.

functionality at C4 position. At this juncture, dearomatization guided (3 + 2) annulation proceeded cleanly producing densely functionalized cage molecule **10a** in 70% yield as a single diastereomer. A minor amount of other regioisomer **11a** (arising from the initial C6-attack on **2a**) was also formed in 14% yield. Reactions of other pyridinium salts (**2**) also led to the production of **10b–10f** in high yields with moderate regio-selectivity (Scheme 4c). With ester based isoquinolinium salts **11a–11b**, reactions were also successful; however, as indicated above, the concomitant transesterification took place to give **10a** in high yields (Scheme 4d).

To highlight synthetic expediency, a one-pot five-component protocol was established. We recognized that synthesis of isoquinolinium salt proceeds at room temperature while the preparation of pyridinium salts requires an elevated temperature. Such reactivity distinction suggested that these azolium salts can be prepared sequentially and engaged in the synthesis of tertiary amine cage scaffolds by controlling the reaction temperature as depicted in Scheme 5a. First, isoquinoline and ethyl bromoacetate were stirred in ethanol for 2 h at room temperature. Then, 3-cyanopyridine, benzyl bromide, and  $\text{Na}_2\text{CO}_3$  were added and the mixture was heated at 60  $^\circ\text{C}$ , where the desired reaction also proceeded effectively to give **4a** in 71% yield without affecting the regio- and diastereoselectivity.

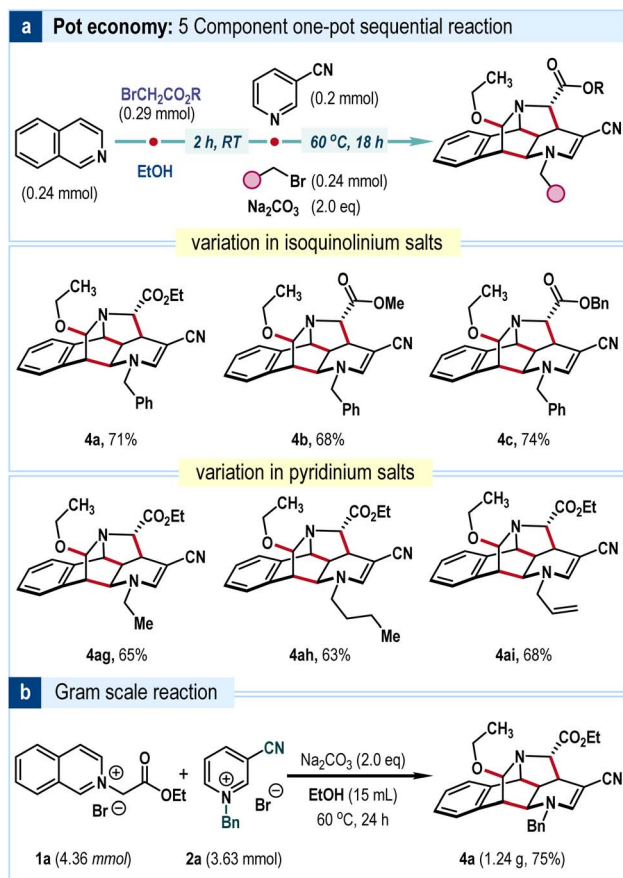
Following the same sequence, various cage scaffolds were also made in good to high yields without compromising selectivities (Scheme 5a). Scale-up was also suitable. A gram-scale reaction rendered **4a** in 75% yield as a single diastereomer with >10 : 1 rr (Scheme 5b).

To gain deeper mechanistic insights, we conducted density functional theory (DFT) calculations (Scheme 6a). The formation of intermediate **A** from the reaction of enolate, generated *in situ* from isoquinolinium salt **1a**, with pyridinium salt **2a** can occur through two distinct pathways: one in which the isoquinoline motif is distal to the nitrile group of the pyridine (blue line), and the other in which the isoquinoline motif is in proximity to the nitrile group of the pyridine unit (red line). Our calculations revealed that the former pathway, with a lower activation barrier ( $\text{TS1}_\text{R} = 4.75 \text{ kcal mol}^{-1}$ ), is more favorable compared to latter ( $\text{TS1}_\text{S} = 5.51 \text{ kcal mol}^{-1}$ ) and it can be attributed to the distabilizing steric interaction of isoquinolinium ring with cyano group of the pyridinium salt. These pathways lead to highly exergonic formation of intermediates **A<sub>R</sub>** and **A<sub>S</sub>**,



Scheme 4 Structural tuning and dearomatization guided (3 + 2) annulation for cage frameworks.

each releasing approximately 15 kcal mol<sup>−1</sup> of energy. Next, the intermediate **A<sub>R</sub>** undergoes a (4 + 2) inverse electron demand Diels–Alder reaction to yield iminium intermediate **B**. It is



Scheme 5 One pot approach and gram-scale reaction.

interesting to note that this (4 + 2) cycloaddition reaction proceeds in a stepwise manner rather than through a concerted mechanism, and the activation barriers for the two carbon-carbon bond formations are 18.18 (**TS2a**) and 5.84 (**TS2b**) kcal mol<sup>−1</sup>, respectively.

Despite numerous attempts, a concerted transition state for the (4 + 2) cycloaddition was not observed. As expected, the subsequent nucleophilic attack of ethanol on the intermediate **B** happens from the less hindered side, which is kinetically more favorable (**TS3<sub>F</sub>**, 4.66 kcal mol<sup>−1</sup> vs. **TS3<sub>C</sub>**, 22.46 kcal mol<sup>−1</sup>), leading to the selective formation of the caged amine product **4a**. Overall, the (4 + 2) cycloaddition step is identified as the rate-limiting step for this reaction (Scheme 6a). When investigating the annulation reaction involving the enolate arising from the isoquinolinium salt **9**, which has an electron-releasing hydroxy group, and the pyridinium salt **2a** (Scheme 6b), we found that the initial nucleophilic attack in both pathways are energetically comparable (**TS1<sub>R</sub><sup>EDG</sup>** = 2.25 kcal mol<sup>−1</sup> vs. **TS1<sub>S</sub><sup>EDG</sup>** = 2.45 kcal mol<sup>−1</sup>). It is only marginally more favorable to produce the intermediate **A<sub>R</sub><sup>EDG</sup>**, where the isoquinoline motif and the nitrile group of pyridine are positioned distally from each other. However, unlike the preceding (4 + 2) annulation reaction, a (3 + 2) annulation predominates here, and it proceeds in a concerted fashion *via*

the **TS<sub>C</sub><sup>EDG</sup>** with an activation barrier of 24.34 kcal mol<sup>−1</sup> to give (3 + 2) cycloaddition product **10a**, which is exothermic by −34.96 kcal mol<sup>−1</sup>. The (3 + 2) cycloaddition step is also the rate-limiting step for this annulation, as apparent from Scheme 6b.

## Conclusions

In summary, we have demonstrated a novel cascade strategy featuring an unexplored intermolecular annulated coupling of two distinct azolium salts derived from isoquinoline and pyridine heterocycles. This innovative approach effectively transforms flat 2D N-heterocycles into complex 3D molecular frameworks with regio- and diastereoselectivity, facilitating the synthesis of challenging caged tertiary amines. By capitalizing on the inherent reactivity of these azolium salts and maximizing their reactive sites, we expedite a double dearomatization-guided (4 + 2) or (3 + 2) annulation reaction, yielding intricate nitrogen-caged motifs, including aza-polycyclic cores akin to hetisine-type alkaloids, in high yields. DFT studies have provided insights into the underlying mechanism of the reaction, revealing that the annulation step is rate-limiting, where (4 + 2) annulation proceeds in a stepwise fashion while corresponding (3 + 2) annulation follows a concerted reaction pathway. To further streamline the synthetic process, we developed a five-component one-pot sequential addition strategy. Importantly, these maneuvers maintain the selectivity of the reaction while emphasizing the efficient utilization of resources (formation of two new rings and four new bonds) and the pot economy. Applications of this concept to access other three-dimensional high-value scaffolds are currently ongoing in our laboratory.

## Data availability

General information, experimental procedures, characterization data for all new compounds, and NMR spectra are in the ESI.† Data for the crystal structure reported in this paper have been deposited at the Cambridge Crystallographic Data Centre (CCDC) under the deposition number CCDC: 2190610.

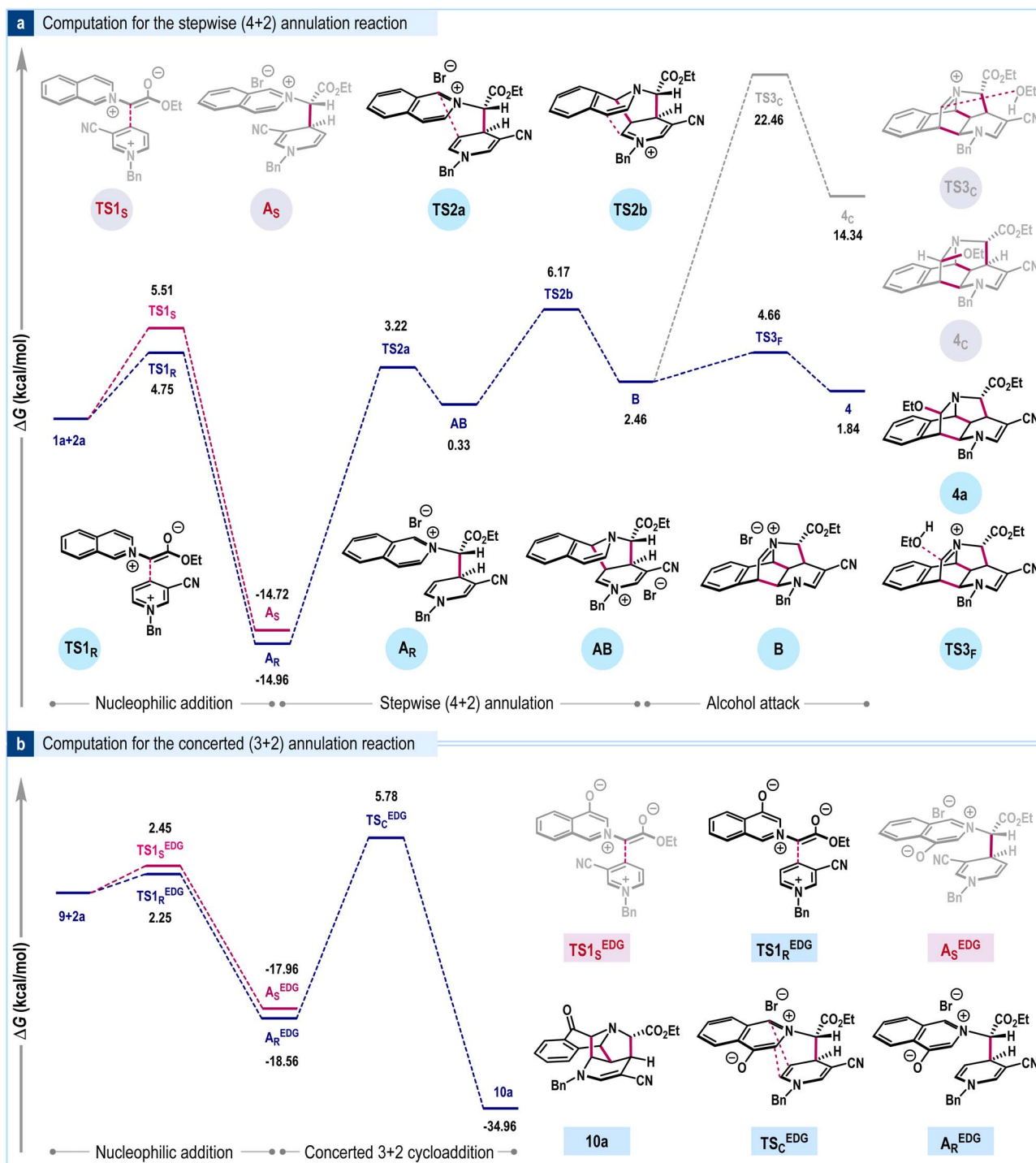
## Author contributions

The manuscript was written through contributions of all authors. All authors have given approval to the final version of the manuscript. M. B. and K. P. have conceptualized the idea. K. P., S. D., S. M. and S. M. carried out the experiments, mechanistic investigations, and analyzed experimental data. V. S. K. C. and V. S. conducted the computational studies. All the authors discussed the results and co-wrote the manuscript.

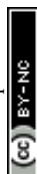
## Conflicts of interest

There are no conflicts to declare.





**Scheme 6** Mechanistic investigation through DFT study. <sup>a</sup>All the quantum chemical calculations were performed using Gaussian 16 program package, employing the density functional theory (DFT) based M062X functional in conjunction with 6-31G(d,p) basis set. Geometries were fully relaxed in solvent (methanol) medium using polarized continuum model (PCM) and characterized by frequency analysis to confirm they are true minima or saddle points on potential energy surface. Relative free energies are given in kcal mol<sup>-1</sup>.



## Acknowledgements

K. P. acknowledges the PMRF fellowship from MHRD, Government of India. We gratefully acknowledge IIT Madras ERP-project (RF23241505CYRFER008650) and IOE-project SB20210792CYMHRD008189) for the financial support.

## Notes and references

- For selected reviews, see: (a) W. C. Wertjes, E. H. Southgate and D. Sarlah, *Chem. Soc. Rev.*, 2018, **47**, 7996–8017; (b) A. R. Pape, K. P. Kaliappan and E. P. Kündig, *Chem. Rev.*, 2000, **100**, 2917–2940; (c) C. J. Huck and D. Sarlah, *Chem.*, 2020, **6**, 1589–1603; (d) C. Zheng and S.-L. You, *ACS Cent. Sci.*, 2021, **7**, 432–444; (e) Y.-Z. Cheng, Z. Feng, X. Zhang and S.-L. You, *Chem. Soc. Rev.*, 2022, **51**, 2145–2170; (f) M. Escolano, D. Gaviña, G. Alzueta-Piña, S. Díaz-Oltra, M. Sánchez Roselló and C. d. Pozo, *Chem. Rev.*, 2024, **124**, 1122–1246. For selected examples, see: ; (g) M. W. Gribble Jr, S. Guo and S. L. Buchwald, *J. Am. Chem. Soc.*, 2018, **140**, 5057–5060; (h) J. Ma, S. Chen, P. Bellotti, R. Guo, F. Schäfer, A. Heusler, X. Zhang, C. Daniliuc, M. K. Brown, K. N. Houk and F. Glorius, *Science*, 2021, **371**, 1338–1345; (i) Z. Siddiqi, T. W. Bingham, T. Shimakawa, K. D. Hesp, A. Shavnya and D. Sarlah, *J. Am. Chem. Soc.*, 2024, **146**, 2358–2363.
- (a) F. Lovering, J. Bikker and C. Humblet, *J. Med. Chem.*, 2009, **52**, 6752–6756; (b) F. Lovering, *MedChemComm*, 2013, **4**, 515–519; (c) K. E. Prosser, R. W. Stokes and S. M. Cohen, *ACS Med. Chem. Lett.*, 2020, **11**, 1292–1298.
- For selected books, see: (a) G. L. Adams and A. B. Smith, *The Chemistry of the Akuammiline Alkaloids*, Elsevier Ltd, 2016; (b) T. Yin, H. Zhang, W. Zhang and Z. Jiang, *RSC Adv.*, 2021, **11**, 36023–36033; (c) N. A. Doering, R. Sarpong and R. W. Hoffmann, *Angew. Chem., Int. Ed.*, 2020, **59**, 10722–10731. For selected examples, see: ; (d) Y. Yasui, T. Kinugawa and Y. Takemoto, *Chem. Commun.*, 2009, 4275–4277; (e) H. Arai, Y. Hirasawa, A. Rahman, I. Kusumawati, N. Cholies, S. Sato, C. Aoyama, J. Takeo and H. Morita, *Bioorg. Med. Chem.*, 2010, **18**, 2152–2158; (f) R. Eckermann, M. Breunig and T. Gaich, *Chem.–Eur. J.*, 2017, **23**, 3938–3949; (g) X. Zong, X. Yan, J. Wu, Z. Liu, H. Zhou, N. Li and L. Liu, *J. Nat. Prod.*, 2019, **82**, 980–989; (h) M. M. Pompeo, J. H. Cheah and M. Movassaghi, *J. Am. Chem. Soc.*, 2019, **141**, 14411–14420.
- For selected books, see: (a) A. Berkessel and H. Groger, *Asymmetric Organocatalysis – From Biomimetic Concepts to Applications in Asymmetric Synthesis*, 2005; (b) C. E. Song, *Cinchona Alkaloids in Synthesis and Catalysis: Ligands, Immobilization and Organocatalysis*, Wiley, 2009. For selected review, see:; (c) A. G. Doyle and E. N. Jacobsen, *Chem. Rev.*, 2007, **107**, 5713–5743.
- For selected Reviews, see: (a) A. M. Hamlin, J. K. Kisunzu and R. Sarpong, *Org. Biomol. Chem.*, 2014, **12**, 1846–1860; (b) A. Hager, N. Vrieling, D. Hager, J. Lefranc and D. Trauner, *Nat. Prod. Rep.*, 2016, **33**, 491–522. For selected examples, see: ; (c) M. Zhang, X. Huang, L. Shen and Y. Qin, *J. Am. Chem. Soc.*, 2009, **131**, 6013–6020; (d) A. M. Hamlin, F. D. J. Cortez, D. Lapointe and R. Sarpong, *Angew. Chem., Int. Ed.*, 2013, **125**, 4954–4957; (e) B. D. Horning and D. W. C. Macmillan, *J. Am. Chem. Soc.*, 2013, **135**, 6442–6445; (f) R. Eckermann, M. Breunig and T. Gaich, *Chem. Commun.*, 2016, **52**, 11363–11365; (g) S. Cathafoline, J. Moreno, E. Picazo, L. A. Morrill, J. M. Smith and N. K. Garg, *J. Am. Chem. Soc.*, 2016, **138**, 1162–1165; (h) X. Xie, B. Wei, G. Li and L. Zu, *Org. Lett.*, 2017, **19**, 5430–5433.
- For selected reviews, see: (a) J. A. Bull, J. J. Mousseau, G. Pelletier and A. B. Charette, *Chem. Rev.*, 2012, **112**, 2642–2713; (b) S. Sowmiah and J. M. S. S. Esperança, *Org. Chem. Front.*, 2018, **5**, 453–493; (c) Y. Xie and Q. Wang, *Org. Biomol. Chem.*, 2021, **19**, 3960–3982; (d) S. Das, *Org. Biomol. Chem.*, 2022, **20**, 1838–1868; (e) N. Kratena and T. J. Donohoe, *Chem. Sci.*, 2022, **13**, 14213–14225. For selected examples, see: ; (f) R. B. Gupta and R. W. Franck, *J. Am. Chem. Soc.*, 1987, **1**, 5393–5403; (g) J. Llaveria, D. Leonori and V. K. Aggarwal, *J. Am. Chem. Soc.*, 2015, **137**, 10958–10961; (h) J. H. Xu, S. C. Zheng, J. W. Zhang, X. Y. Liu and B. Tan, *Angew. Chem., Int. Ed.*, 2016, **55**, 11834–11839; (i) B. M. Reeves, H. B. Hepburn, A. Grozavu, P. J. Lindsay-scott and T. J. Donohoe, *Angew. Chem., Int. Ed.*, 2019, **58**, 15697–15701; (j) D. Zhang, Z. Su, Q. He, Z. Wu, Y. Zhou, C. Pan, X. Liu and X. Feng, *J. Am. Chem. Soc.*, 2020, **142**, 15975–15985; (k) C. McLaughlin, J. Bitai, L. J. Barber, A. M. Z. Slawin and A. D. Smith, *Chem. Sci.*, 2021, **12**, 12001–12011; (l) Y. Lu, P. N. Dey and C. M. Beaudry, *Chem.–Eur. J.*, 2021, **27**, 4028–4032; (m) M. Kischkewitz, B. Marinic, N. Kratena, Y. Lai, H. B. Hepburn, M. Dow, K. E. Christensen and T. J. Donohoe, *Angew. Chem., Int. Ed.*, 2022, **61**, e202204682; (n) J. C. Abell, C. P. Bold, L. Vicens, T. Jentsch, N. Velasco, J. L. Tyler, R. N. Straker, A. Noble and V. K. Aggarwal, *Org. Lett.*, 2023, **25**, 400–404; (o) A. J. N. Lamhauge, D. A. Mcleod, L. Casper, G. A. Oliver, L. Viborg, T. Warburg and K. A. Jørgensen, *Chem.–Eur. J.*, 2023, e202301830.
- For reviews, see: (a) W. C. Wertjes, E. H. Southgate and D. Sarlah, *Chem. Soc. Rev.*, 2018, **47**, 7996–8017; (b) J. M. Saya, E. Ruijter and R. V. A. Orru, *Chem.–Eur. J.*, 2019, **25**, 8916–8935; (c) C. J. Huck, Y. D. Boyko and D. Sarlah, *Nat. Prod. Rep.*, 2022, **39**, 2231–2291; (d) M. Zhu, X. Zhang, C. Zheng and S. L. You, *Acc. Chem. Res.*, 2022, **55**, 2510–2525. For a selected example, see: ; (e) J. Ma, F. Strieth-Kalthoff, T. Dalton, M. Freitag, J. L. Schwarz, K. Bergander, C. Daniliuc and F. Glorius, *Chem.*, 2019, **5**, 2854–2864; (f) H. J. Miao, L. Le Wang, H. Bin Han, Y. De Zhao, Q. L. Wang and Z. W. Bu, *Chem. Sci.*, 2020, **11**, 1418–1424; (g) J. K. Kerkovius, A. Stegner, A. Turlik, P. H. Lam, K. N. Houk and S. E. Reisman, *J. Am. Chem. Soc.*, 2022, **144**, 15938–15943; (h) B. Singh, A. J. Ansari, N. Malik and S. S. V. Ramasastry, *Chem. Sci.*, 2023, **11**, 6963–6969.
- (a) K. M. Peese and D. Y. Gin, *J. Am. Chem. Soc.*, 2006, **128**, 8734–8735; (b) K. M. Peese and D. Y. Gin, *Chem.–Eur. J.*, 2008, **14**, 1654–1665. For intermolecular reports, but not explored toward caged-amine scaffolds, see: ; (c)



- A. R. Katritzky and Y. Takeuchi, *J. Am. Chem. Soc.*, 1970, **92**, 4134–4136; (d) A. R. Katritzky and N. Dennis, *Chem. Rev.*, 1989, **89**, 827–861; (e) M. E. Jung, L. M. Zeng, T. S. Peng, H. Y. Zeng, Y. Le and J. Y. Su, *J. Org. Chem.*, 1992, **57**, 3528–3530; (f) V. C. Pham and J. L. Charlton, *J. Org. Chem.*, 1995, **60**, 8051–8055; (g) W. Sliwa, *Heterocycles*, 1996, **43**, 2005–2029; (h) M. J. Sung, H. I. Lee, Y. Chong and J. K. Cha, *Org. Lett.*, 1999, **1**, 2017–2019; (i) H. I. Lee, M. J. Sung, H. B. Lee and J. K. Cha, *Heterocycles*, 2004, **62**, 407–422.
- 9 For a book, see: (a) *Domino Reactions: Concepts for Efficient Organic Synthesis*, ed. L. F. Tietze, Wiley-VCH, Weinheim, 2014. For Reviews, see:; (b) K. C. Nicolaou, T. Montagnon and S. A. Snyder, *Chem. Commun.*, 2003, **3**, 551–564; (c) E. C. Cherney and P. S. Baran, *Isr. J. Chem.*, 2011, **51**, 391–405; (d) R. Ardkhean, D. F. J. Caputo, S. M. Morrow, H. Shi, Y. Xiong and E. A. Anderson, *Chem. Soc. Rev.*, 2016, **45**, 1557–1569.
- 10 Y. Hayashi, *Acc. Chem. Res.*, 2021, **54**, 1385–1398.

